ZANCO Journal of Pure and Applied Sciences

TYPE Original Research
DOI http://dx.doi.org/10.21271/ZJPAS.36.4.4

OPEN ACCESS

*CORRESPONDENCE
Shaida Anwer Kakil
shaida.kakil@su.edu.krd

RECEIVED 26/02/2024
ACCEPTED 24 /05/ 2024
PUBLISHED 31/08/ 2024

KEY WORDS:
Hydroxyapatite; Femur bone and ribs; Gamma irradiation; Mass attenuation coefficients.; NIST XCOM

Effect Gamma-ray on structure and mass attenuation coefficient of Hydroxyapatite $Ca_{10}(PO_4)_6(OH)_2$, in Bovine Bone

Rozhan Dilshad Haider[1], Mohammed Issa Hussein[1], Shaida Anwer Kakil [1]

1Department of Physics, College of Science ,Salahaddin University-Erbil, Erbil, Kurdistan Region, Iraq.

Abstract:

Hydrothermal treatment procedures were employed, to generate hydroxyapatite ($Ca_{10}(PO_4)_6(OH)_2$,(HAP) powder, from the femur and ribs of bovine bone samples. This investigation delves into the effect of gamma rays, from a Cs-137 activity equal to 220 µCi at integral doses of 20 kGy, on the surface structures, vibration properties, and attenuation coefficient of HAP, in the bovine femur bone and ribs. The mass attenuation coefficients for HAP powder were registered as E= 511 keV, with 1276 keV gamma energy released from the 22Na radioisotope, and 662 keV gamma energy released from the 137Cs radioactive isotope. We used the Nist XCom program to calculate the mass attenuation coefficient of HAP before and after radiation for photon energies ranging from 0 keV to 100 keV.

1.Introduction

The mechanical properties of bone, including its resistance to fracture, sturdiness, and ductility, are influenced by its intricate collagen arrangement, HAP, and water content (Rahman et al., 2018). Hydroxyapatite (HAP) is a calcium phosphate mineral with the chemical formula Ca1010(PO44)66(OH)22, known for its close resemblance to the inorganic component of bone and teeth. HAP is widely used in biomedical applications such as bone grafts, dental implants, and orthopedic devices due to its biocompatibility and osteoconductivity. (Bano et al., 2017). Numerous studies have been published over the last decade exploring various methods for preparing and processing hydroxyapatite (HA) bioceramics. Solid-state synthesis of HA (Kien et al., 2018), typically from oxide or inorganic salt powders, involves extensive mechanical mixing and prolonged heat treatments at high temperatures. These methods, while effective, often present challenges in controlling the microstructure, grain size, and grain size distribution of the resulting powders or components. Wet-chemical and soft chemistry (Yelten-Yilmaz and Yilmaz, 2018) approaches offer alternatives with greater flexibility in processing. and spray- or gel-pyrolysis (Bogdanoviciene et al., 2006) have been employed to create HA phases. Despite their benefits, many of these methods are complex and time-consuming, and can suffer from inconsistencies in solution behavior among the various chemical constituents.

The chemical components and biological configuration of HAP, which are influenced by a variety of natural bone parameters (Fiume et al., 2021), have attracted stakeholders in the industrial and medical fields' attention(George et al., 2020, Amenaghawon et al., 2022). In the context of its dry weight molecular composition, animal bone is made up of between 30% to 35% organic elements, and between 65% to 70% inorganic elements. The bone's organic portion comprises mostly collagen (95%) and proteins, as well as chondroitin sulphate, keratin sulphate, and a variety of lipids including phospholipids, cholesterol, fatty acids, and triglycerides. As for the bone's inorganic portion, this is made up mainly of HAP, which is essentially a calcium/phosphate-based bio ceramic, generally expressed as $Ca_{10}(PO_4)_6(OH)_2$. In terms of chemical composition, HAP is identical to the inorganic component of the bone matrix (an exceedingly intricate bone constituent) (Malla et al., 2020, Bano et al., 2017). For the most part, regular HAP materials are derived from bovine bone (Ghedjemis et al., 2022, Osuchukwu et al., 2021) . Sandra M. et al investigated the thermal, resonance, structural, and morphological changes of hydroxyapatite derived from swine bone (Unal et al., 2021, Londoño-Restrepo et al., 2016) . While the sintering of HAP at high temperatures (exceeding 1000^oC) delivers reduced ionic reactivity and cytotoxicity towards bone cells, the downside to this step comes in the form of substantially diminished ceramic granule porosity (Borkowski et al., 2020, Forero-Sossa et al., 2021).

Over the past few years, the growing involvement of radioactive elements in the realms of medicine, tomography, gamma-ray fluorescence investigations, radiation biophysics, the nuclear industry, space research and agriculture among others, has led to the emphasis on issues associated to the photon atom interaction parameters, which include attenuation and absorption coefficients, as well as photon interaction cross-section in materials (Sidhu et al., 2012, Akça et al., 2022). Attenuation is defined as the deletion of photons from the gamma ray beam, during its passage through a material. The occurrence of attenuation is brought about by the absorption and dispersal of primary photons. The portion of photons deleted, for each unit thickness of the material, from a mono-energetic beam of gamma ray, is referred to as the linear attenuation coefficient. The likelihood of interaction, for a specified thickness, is influenced by the atom count for each volume. To surmount dependence on the material, the linear attenuation coefficient is rendered normal, by splitting the material density, to derive the mass attenuation coefficient (Rafiei et al., 2022). In a study conducted by Sepideh Yazdani et al, the NIST-XCOM programme was harnessed, to hypothetically compute the mass attenuation coefficient, with regards to distinct for some body

tissues (Yazdani Darki et al., 2020). While the therapeutic value of ionizing radiation, as a treatment for cancer, is well established, its usage comes with certain drawbacks, particularly in the context of routine bone function failure, and tissue death. As such, from a clinical standpoint, it is imperative that the issues, triggering these iatrogenic problems, be thoroughly investigated (Tiwari and Mishra, 2020) . High doses of radiation bring about necrosis in the cells of soft tissues, while lower doses instigate apoptosis. A brief investigation was conducted, to ascertain the response of bone cells, to high and low doses of radiation (Ajith Kumar et al., 2023). Other than damaging the mechanical properties of bone, to render it more breakable, gamma radiation also alters the bone's surface properties. Previous studies have revealed that in a situation where the surface of a non-irradiated bone sample is heavily mineralized with mineralized osteon fibres, gamma radiation alters its surface features (Rahman et al., 2018). The markedly changing effects of topical irradiation on overripe bone can be put down to alterations in photon energy (Salcedo et al., 2020). It is notable, that few investigations have emphasized on the issue of bone mineralization, in children under treatment for cancer. Although not all children treated for cancer are affected, osteopenia is frequently diagnosed in young adults, who survived cancer during childhood(Marcucci et al., 2019). In a study conducted by Kaminski A. et al, the administration of 25 kGy and 35 kGy gamma irradiation doses on human cortical bone, led to the implication of a link, between the mechanical properties of bone tissue grafts, and the deterioration of the collagen structure (Kaminski et al., 2012). This study involves the use of the hydrothermal extraction method to synthesize natural HAP from bovine bones, followed by calcination at a range of temperatures. This extraction method facilitates the thermal decomposition and removal of organic components in bones. The experimental and theoretical measurements of the half-value thicknesses, as well as the linear and mass attenuation coefficients of biological hydroxyapatite Ca10(PO4)6(OH)2 in bone, were performed with the use of 22Na and 137Cs gamma-ray point sources. Furthermore, by administering a 20 kGy dose rate, we investigated the influence of gamma radiation on HAP. A variety of methods, including scanning electron microscopy (SEM), energy-dispersive X-ray spectroscopy (EDX), and Fourier transform infrared spectroscopy (FT-IR), were employed to characterize the samples prior to and after gamma irradiation.

2.MATERIALS AND METHODS

2.1 Experimental

2.1.1 Formulation of hydroxyapatite (Ca10(PO4)6(OH)2) from bone

The process of formulating hydroxyapatite (HA) from bone involves converting raw bone into a pure form of calcium phosphate. This typically requires removing organic components, treating the bone material, and ensuring the resulting hydroxyapatite has the desired physical properties.To obtain the required material, rib and femur bones from male bovines, aged 6 to 12 months, were sourced from an abattoir. The bones underwent a preliminary boiling in water for one hour to remove macroscopic impurities. After boiling, they were thoroughly washed and rinsed multiple times with water to ensure complete removal of meat remnants, tendons, bone marrow, and other soft tissues. Following this initial cleaning, the bones were immersed in acetone for two hours to extract any remaining fat and grease. They were then rinsed with distilled water to ensure that any residual acetone and fat were completely removed. This preparation method is a key step in creating a clean base for further processing into hydroxyapatite.

The hydrothermal technique was employed for the generation and extraction of HAP from the bones after heated in a furnace at 600 to 1000^{o} C to completely remove organic matter from the bone and provide hydroxyapatite our result agree with (Akram et al., 2014). This can be considered a more trouble-free and safer means, for HAP extraction, compared to other chemical-based technique (Agrawal et al., 2011, Barakat et al., 2009). The formulation process for the hydroxyapatite $Ca_{10}(PO_4)_6(OH)_2$ powder disk in bone is presented in Fig. 1. Following the

selection of the bovine femur and rib cortical bones, the soft tissues, periosteum, the medullary fragment of the bone, and bone marrow were discarded. The utilization of the Archimedes density technique (Akar et al., 2006, Gunduz et al., 2008), revealed the hydroxyapatite densities of the femur bone, and ribs cortical bone for four models; the femur and ribs hydroxyapatite before and after radiation at room temperature,the water density was registered as 0.997 g/cm^3 (Singh et al., 1998).

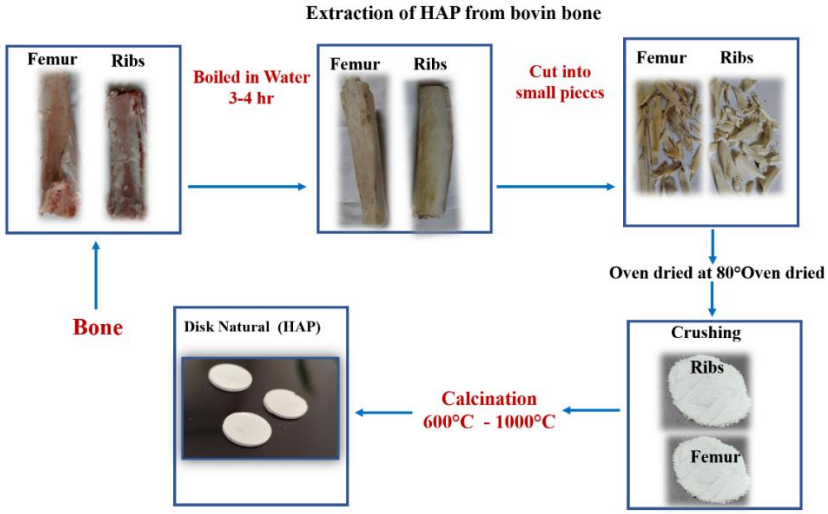

Figure 1. Formulation of the hydroxyapatite $Ca_{10}(PO_4)_6(OH_{)2}$ powder disk

2.1.2 Characterizations of the of the hydroxyapatite Ca10(PO4)6(OH)2 powder disk

Energy-dispersive X-ray spectroscopy (EDS), conducted using a Bruker nano detector (XFlash 5010), was employed to analyze the elemental composition of bone samples at various temperatures. To characterize the hydroxyapatite (Ca10(PO4)6(OH)2), including its particle size and morphology, field-emission scanning electron microscopy (FE-SEM) using a Quanta 4500 system was utilized. Additionally, Fourier-transform infrared (FT-IR) spectroscopy, using a JASCO FT/IR-4600 system, was performed to examine the chemical bonds and identify functional groups in the hydroxyapatite. These techniques provided a comprehensive understanding of the composition, structure, and characteristics of the hydroxyapatite derived from bone.

2.1.3 Attenuation coefficient measurement

A gamma spectrometer, equipped with a scintillation detector (SILENA type model 3S3), was employed for this study. The testing process involves the use of a NaI(Tl) detector (3 × 3), with an energy resolution of 7.4%, at 662 keV gamma rays, from the decay of ^{137}Cs (Fig. 2). The detector, which is protected by lead collimators, to deter the encroachment of scattered radiation from nearby objects, absorbs a slender beam of gamma ray channelled through the material. The calibration of the gamma spectroscopy system is performed with the use of ^{241}Am, ^{137}Cs, ^{22}Na and ^{60}Co gamma sources. A multi-channel analyser (512), with Cassy software, was employed to keep count of the transmitted gamma ray signals. The potency of mono-energetic photons, with energies 511 and 1276 keV for 0.02 mCi ^{22}Na, and 661 keV for 0.1mCi ^{137}Cs, were measured for the samples. The gamma spectroscopy procedure was harnessed, to ascertain the intensity of incident photons (I_o), and the intensity of gamma rays, passed through the sample sans interaction (I). The computation, for the peak locations, is based on the spectrum acquired for each measurement. The counting time for the discs was set to 200 s for ^{22}Na and ^{137}Cs. The span between the standard γ-point source, and the sample, was set as 4.7 cm, while the span

between the γ-point, and the detector was set as (6.5cm). The mass was fixed for all of the samples, and the regular thickness of the discs was ensured. The mass attenuation coefficients of all hydroxyapatite samples were computed as shown in Fig. 10 and 11 prior and after 20 kGy, and also calculated theoretically using the XCOM program in several gamma energies of current.

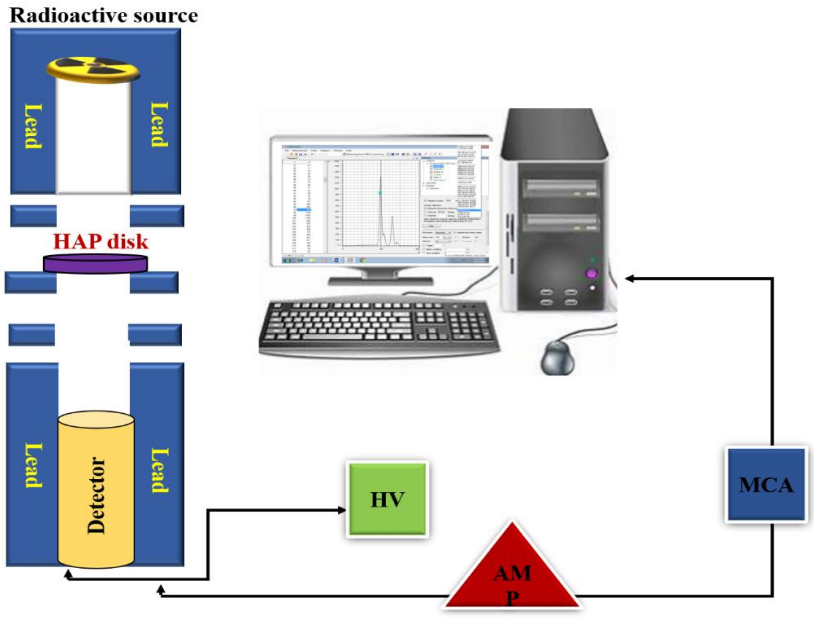

Figure 2. Measurement of attenuation coefficient

2.2 Theoretical approaches: NistXCom

A diagram depicting the approach adopted by this study, for measuring the attenuation coefficient, is exhibited in Fig. 10. The computation, for the photon interaction parameter in hard tissue, was conducted with the use of NistXCom programmes developed by (Berger and Hubbell, 1987). The attenuation of photons, travelling through matter, is attributed to absorption, and scattering activities. Attenuation caused by absorption is in agreement with the Beer–Lambert's law

$$I = I_0 e^{-\mu x} \quad \text{.....1}$$

in which I_0 and I represent the photon intensities, while μ represents the photon attenuation coefficient (cm^{-1}). The NistXCom programme code is applied, to compute the values of mass attenuation coefficient (μ_ρ, cm^2 /g), for all aspects and intricate materials, in accordance with the mixture rule, at any level of energy, ranging between 1 keV to 100 GeV (Hubbell and Seltzer, 1995, More et al., 2016).

$$(\mu/\rho)_C = \sum w_i (\mu/\rho)_i \quad \text{.....2}$$

in which w_i and $(\mu/\rho)_i$ represent the weight fraction and photon mass attenuation coefficient of the *i*th constituent element, respectively. In the case of a chemical compound, the fraction by weight (w_i) is expressed as:

$$w_i = \frac{n_i A_i}{\sum n_j A_j} \quad \text{.....3}$$

whereby A_i represents the atomic weight of the *i*th element, and *ni* represents the sum of formula units (Koksal et al., 2019).

3.RESULTS AND DISCUSSION

3.1 Characteristic molecular vibration by using FT-IR spectroscopy

FT-IR spectroscopy is regarded as an indispensable characterization option, for the identification of functional groups, existing in femur and rib bone powder, prior to radiation. The powders were heated at temperatures of 600°C, 800°C and 1000°C, prior to radiation with 20 kGy. This process is illustrated in Figures 3 and 4

As indicated by the characteristic bands of

hydroxyapatite, the femur and rib bone powders, prior to heating, are similar in terms of FT-IR spectra, albeit with slight disparities in intensity and wave number, for certain functional groups

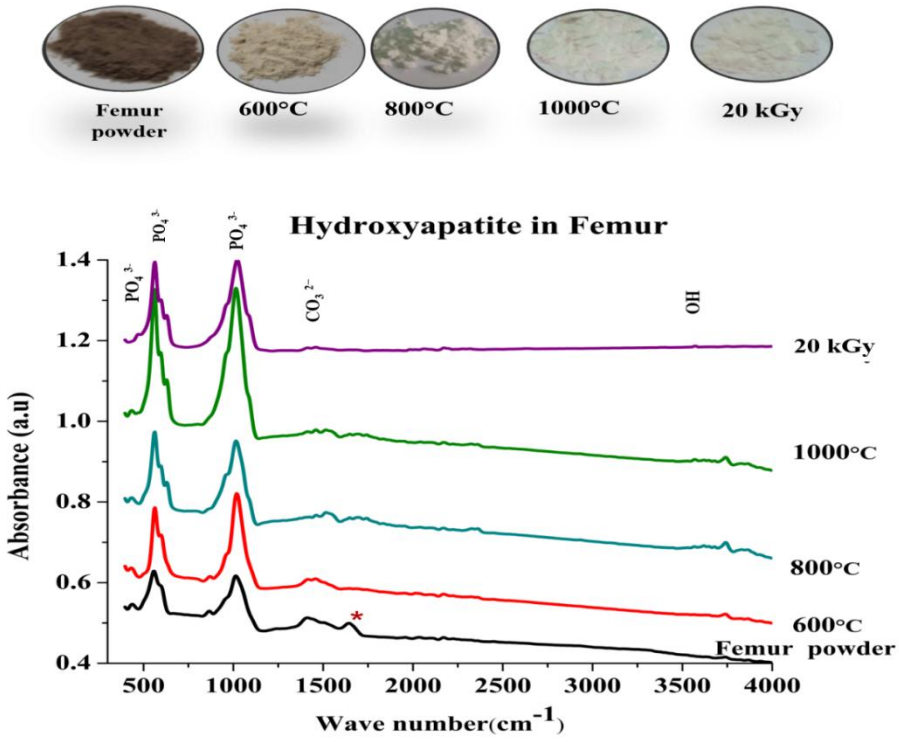

Figure 3. FT-IR for raw bone powder sample (femur): prior to radiation, following heating at 600,800 and 1000 °C for 3 h, and after radiation with 20 kGy.

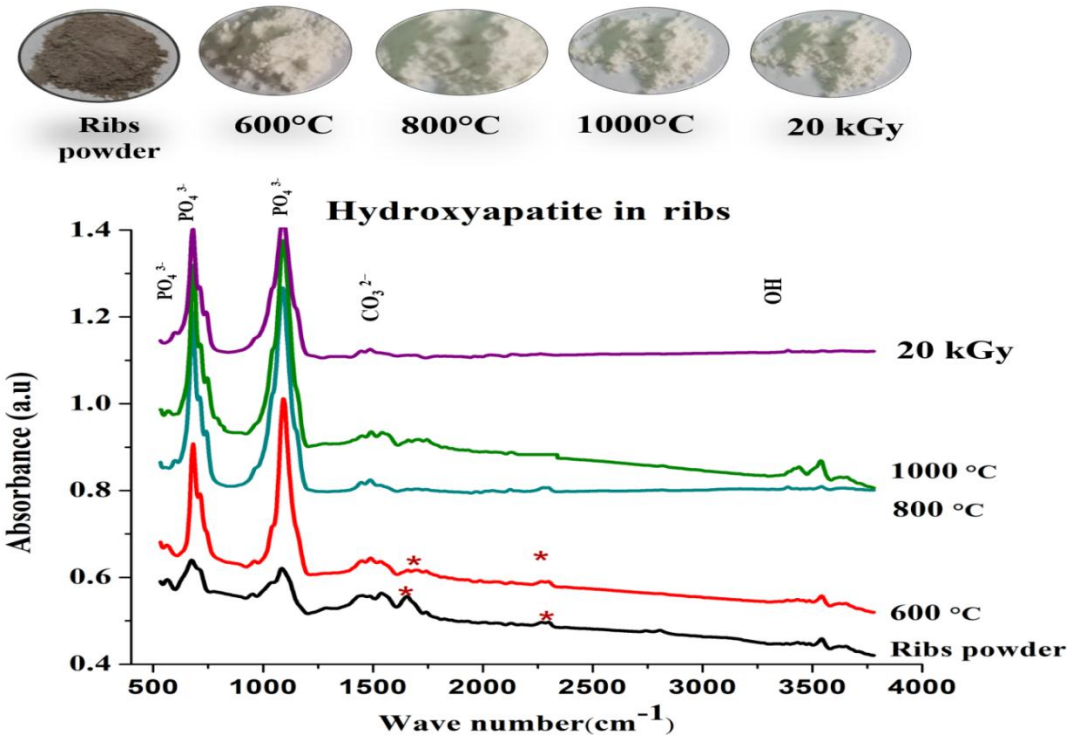

Figure 4. FT-IR for raw bone powder sample (ribs): prior to radiation, following heating at 600,800 and 1000 °C for 3 h, and after radiation with 20 kGy.

The bands at (3741, 3571, and 3741) cm^{-1}, (3741, 3741, and 3733) cm^{-1} for femur and ribs respectively, are attributable to OH stretching. These bands are not discerned following 20 kGy gamma radiation. The peaks at (1645) cm^{-1} for femur, and (1628) cm^{-1} for rib powder, as signified by (*), are consistent with the amide group. The peaks for femur powder and rib powder were eradicated, following heating at 600^{o}C and 800^{o}C respectively. The peak at 2349.32 cm^{-1}, consistent with NH, discerned in rib powder, was removed following heating at 800^{o}C. As portrayed in the inset of Fig.s 3 and 4, this can be visually verified through the color change from grey to white. The change in color for the femur and rib bones, from grey-brown to white, occurred at the heating temperatures of 600^{o}C and 800^{o}C respectively. The initial CO_2 discharge, transpiring below 500^{o}C, is attributed to organic component combustion, while the subsequent portion of CO_2 discharge, transpiring above 500^{o}C corresponds to structural carbonate loss (Mamede et al., 2018). A three-hour heating period, at 1000^{o}C, led to the sample turning fully white. This verifies the development of a calcium phosphate compound or the hydroxyapatite. Similarly, in a study conducted by Odusote, pure hydroxyapatite was derived from bovine bone, after its heating at 700^{o}C, for a period of 6 hours (Odusote et al., 2019). The bands at 1438cm^{-1} and 1489 cm^{-1} for the rib and femur bone powder respectively, are attributable to the carbonate group (CO_3^{2-}). Following radiation, the area curve declined. These results agree with those derived from an investigation conducted Gomes and colleagues (Gomes et al., 2021). The absorption bands at approximately 570 cm^{-1}, and the distinct peak at roughly 1026 cm^{-1}, are attributed to the bending and stretching vibration modes, of the v4 PO_4^{3-} groups and v1, v3 PO_4^{3-} band respectively. The v1, v3 PO_4^{3-} band peak, at about 1026 cm^{-1}, was rendered more pointed, with the increase in temperature. However, it was rendered less pointed, following radiation. Also, due to the extension in bond length, the v4PO_4^{3-}, at the approximately 559 cm^{-1}region, was rendered frailer, and transferred to a lesser wave number. The alterations, in bond length, can be attributed to electronegativity variations, in the adjacent atom (Wang et al., 2019). The inconsequential peak, situated at roughly 422 cm^{-1}, is in keeping with v2 PO_3^{4-}. This agrees with the result derived through an investigation conducted by Kourkoumelis et al. However, following radiation, the peak was no longer discernible for both powders (Kourkoumelis et al., 2019).

3.2 Morphology of bovine femur and rib bone powder, hydroxyapatite and prior and after 20 kGy irradiation

The morphology of bovine femur and rib bone powder before and after calcination at 1000^{o}C and hydroxyapatite before and after radiation, is depicted in Fig. 5 and 6 respectively. scanning electron microscopy revealed that exposure to gamma irradiation alters the shape of hydroxyapatite. This observation agrees with (Girija et al., 2008, Predoi et al., 2022). While the unirradiated films were regular and free of indentations, the films irradiated at 20 kGy were grouped into different shapes, and marked with cavities. Descriptions of the alterations, brought about by irradiation, are available in relevant literature (Rana et al., 2017). The groupings and cavities, resulting from irradiation, can be put down to the onset of flaws, initiated by the interaction between gamma ray and the powder. It is essential that future studies in this area, take into consideration the age and food intake of the animals, from which the bones were acquired, as these biological issues, can have a significant influence on the hydroxyapatite SEM results. Fig. 6 shows the SEM: (a) Femur hydroxyapatite powder and (b) Rib hydroxyapatite powder following radiation with 20 kGy. The SEM images of hydroxyapatite at high magnification in the inset of Fig. a and b show the interior particles in red circles. The results show that after magnification of 500 nm, the crystal shape and size of hydroxyapatite ($Ca_{10}(PO_4)_6(OH)_2$) from bovine femur are different compared with hydroxyapatite bovine ribs. It is clear that gamma radiation has a significant impact, affecting various regions that exhibit different shapes and morphologies

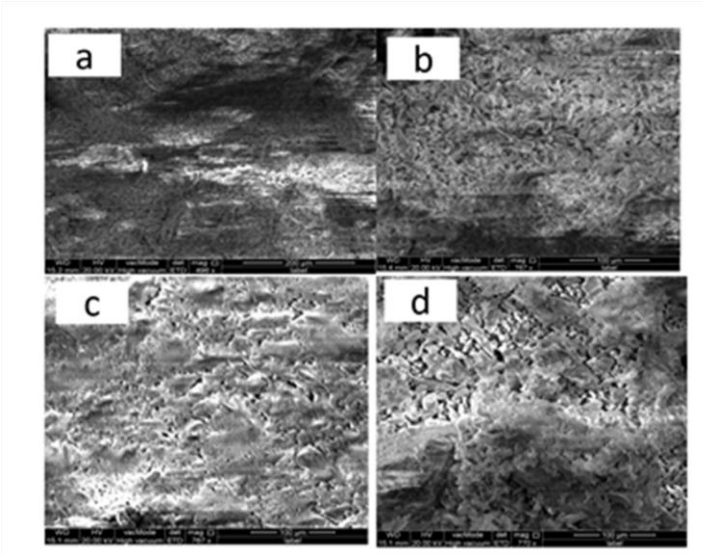

Figure 5. The SEM of (a) Femur powder before calcination, (b) femur hydroxyapatite after calcination1000^{o}C, (c) Rib powder before calcination, and (d) rib hydroxyapatite after calcination1000^{o}C.

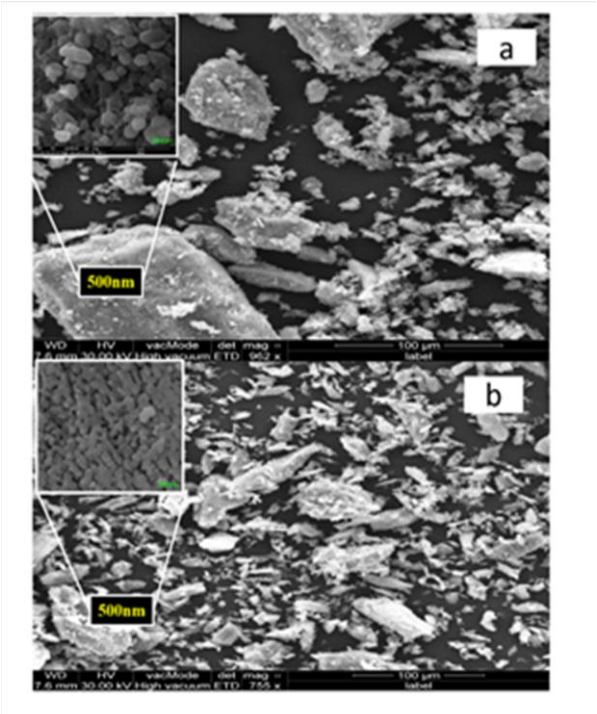

Figure 6. The SEM: (a) Femur hydroxyapatite powder and (b) Rib hydroxyapatite powder following radiation with 20 kGy

3.3 Energy dispersive X-ray investigation (EDX)

An appropriate calcium-to-phosphorus ratio (Ca:P), is essential for favorable bone growth and development, particularly during early childhood. The ideal ratio may differ from one individual to another, depending on gender, age, bone variety, and bone location (Balatsoukas et al., 2010). For our investigation, the ratio of calcium to phosphorous in rat bone was scrutinized, prior to and after gamma radiation. Figures 7 and 8 depict standard EDX spectrums, featuring the different elements existing in the bovine femur and rib bones. For the most part, the Ca/P ratio for both samples is fairly greater than the stoichiometric value of 1.67 (Sobczak-Kupiec and Wzorek, 2012). Annealing at 1000^{o}C, gave rise to the as-received bovine bone Ca/P ratio, of 2.06 for the femur bone, and 2.31 for the rib bone. These results agree with (Ooi et al., 2007), who calculated a Ca/P ratio of 2.03, for hydroxyapatite extracted from bovine femur bone. Additional radiation administration led to a dip in the Ca/P ratio to approximately 1.9 for the femur bone, and 2.046 for the rib bone. As illustrated in Fig. 9, radiation substantially alters the Ca/P ratio.

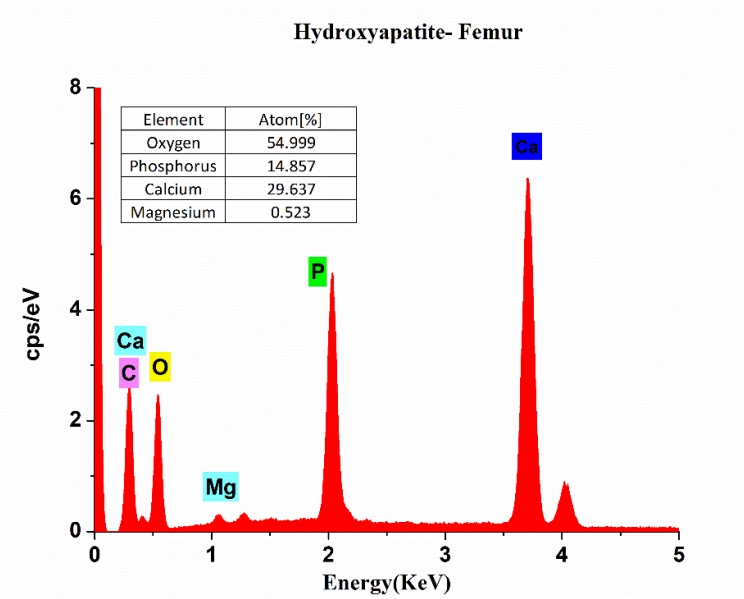

Figure 7. EDX assessment of hydroxyapatite, deriving from a bovine femur bone.

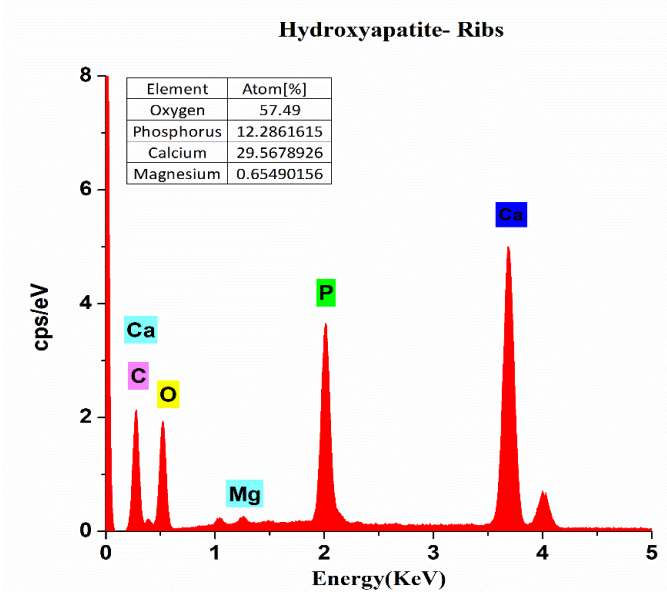

Figure 8. EDX assessment of hydroxyapatite, deriving from a bovine rib bone.

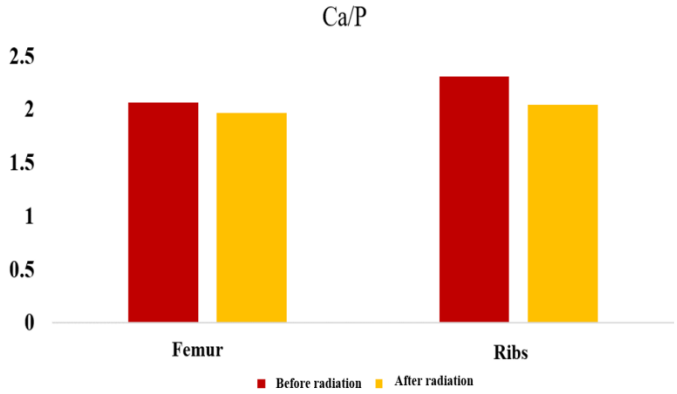

Figure 9. Radiation impact on the Ca/P ratio of hydroxyapatite, deriving from bovine femur and rib bones.

3.4 Irradiated and non-irradiated mass attenuation coefficients of hydroxyapatite, extracted from bovine femur and rib bones

Theoretical mass attenuation coefficients of hydroxyapatite were achieved by the way of NistXCom software. Fig. 10 portrays the mass attenuation coefficient for the real hydroxyapatite $Ca_{10}(PO_4)_6(OH)_2$ system, at different energy levels in the 1 keV–100 GeV range. In the context of total mass attenuation coefficients as functions of energy, three energy occurrences are evident: photoelectric absorption, Compton scattering, and pair production. The mass attenuation coefficient values are high at low energy sides and decrease sharply until 1200 keV. Above 1٢00 keV slight decreases occur in mass attenuation coefficients and it stays almost constant. Although a few literatures studied the effect dose of gamma radiation on the photo-interaction parameter (attenuation coefficient) of different materials experimentally and theoretically; most recently (Dehghani et al., 2018) was observed that after irradiation, the mass attenuation coefficients are reduced to a lesser values and they showed the mass attenuation coefficients of materials are not only depend on the mass atomic number also depend on the Morphology material. Amini et al. studied the effect of gamma radiation on MgO structure and the mass attenuation coefficient, they investigated mass attenuation coefficient not only depends on the effective atomic number but also depends on the size of the particles (Amini et al., 2018). Moreover, in addition, O.K. Koksala studied the assessment of the mass attenuation parameters with using gamma rays for nano hydroxyapatite (Koksal et al., 2019). investigated the radiation sterilization kills the donor bone diseases but it damages the bone mechanical properties and strength but they did not mention on attenuation coefficient (Rahman et al., 2018). According to above literature the relationship between gamma dose and attenuation coefficient has yet to be established, and it was showed the attenuation coefficient not only depend on atomic number, as a result we investigated effect morphology of hydroxyapatite on mass attenuation coefficient before and after 20 kGy dose. Theoretical mass attenuation coefficient values for hydroxyapatite derived from bovine femur and rib bones obtained from the NIST-XCOM database were compared with experimental values of mass attenuation coefficient for non-irradiated hydroxyapatite are shown in Fig.s 11 and 12, these Fig.s represent the computation for mass attenuation coefficients, by the way of gamma spectroscopy procedure, at energy levels of 511 keV, 662 keV, and 1276 keV, prior and after radiation at 20 kGy, is demonstrated. The mass attenuation coefficient of hydroxyapatite, derived from bovine femur and rib bones, as a function of photon energy E = 511 keV, 662 keV, and 1276 keV, was reduced by the rise in gamma-ray energy.

Also, before radiation the mass attenuation coefficient of hydroxyapatite derived from bovine femur and rib bones are different because the Ca/P ratio for hydroxyapatite and morphology from the bovine rib and femur are different. The literature's results agree with the reference (Tariq et al., 2017), It is considered that the electron density can change when the Ca/P is changed after radiation due to the elemental composition of materials. It is also evident that the decreases in mass attenuation coefficients, for the extraction of hydroxyapatite from the bovine rib bone following radiation, is more pronounced than that for the extraction of hydroxyapatite from the bovine femur bone.

The experimental, and theoretical results, indicate that the mass attenuation coefficients of the materials, are not determined by mass atomic number, but by density, and morphology calculated Ca/P ratio by EDX, the reason is that the Ca/P content decreases and it is thought to decrease the mass attenuation coefficient at dose rate equal to 20 kGy. The difference between experimental and theoretical attenuation values appears the incident and transmitted radiation intensity, powder thickness and counting statistics also ratio Ca/P. The results confirm that the experimental value is reliable when compared to the predicted values.

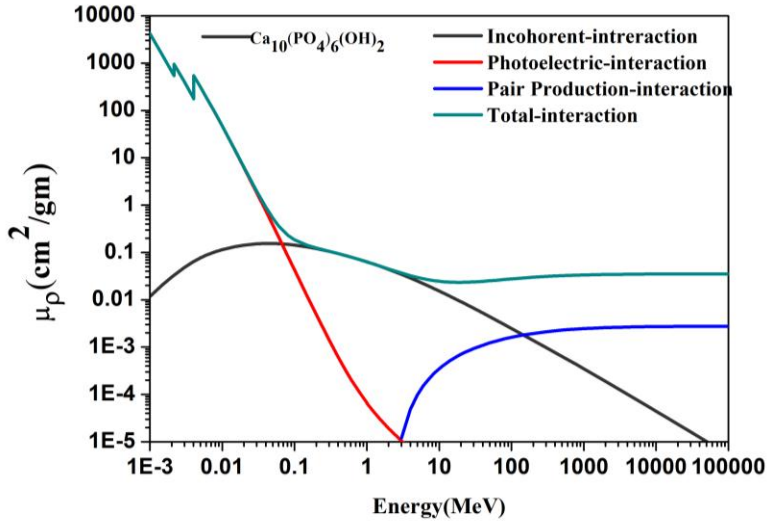

Figure 10. NistXCom computation for mass attenuation coefficient of hydroxyapatite $Ca_{10}(PO_4)_6(OH)_2$, as a function of photon energy, for various collaborations in the 1–100 GeV range.

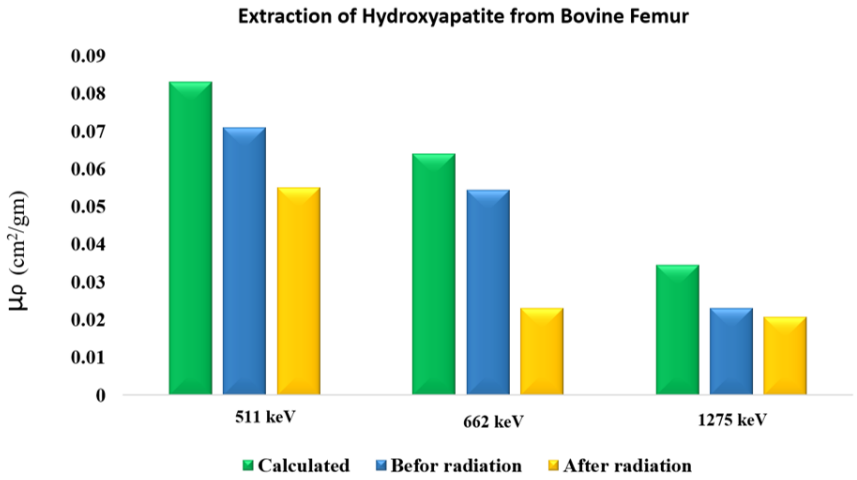

Figure 11. Assessment of mass attenuation coefficient of hydroxyapatite, derived from bovine femur bone, as a function of photon energy E = 511 keV, 662 keV, and 1276 keV, prior and after 20 kGy radiation, with regards to theoretical values.

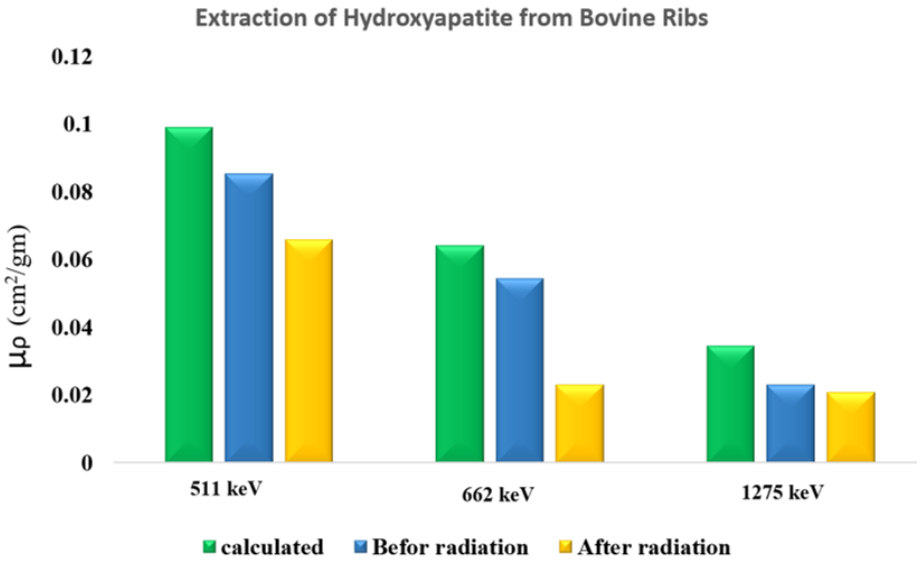

Figure 12. Assessment of mass attenuation coefficient of hydroxyapatite, derived from bovine rib bone, as a function of photon energy E = 511 keV, 662 keV, and 1276 keV, prior and after 20 kGy radiation, with regards to theoretical values.

4.CONCLUSION

For this investigation, SEM, FT-IR spectroscopy, and EDX spectroscopy were employed to characterize synthesized hydroxyapatite. The unadulterated hydroxyapatite from bovine bone was procured through heating at 1000°C for 3 hours and gamma-ray irradiation from a Cs-137 activity equivalent to 220 µCi at integral doses of 20 kGy, administered at room temperature. From this research, the following conclusions can be drawn:

- SEM images showed that the dose of gamma ray affected the shape and size of Hydroxyapatite $Ca_{10}(PO_4)_6(OH)_2$ and agglomerated in different shapes.
- EDX spectroscopy revealed increased surface pore count following irradiation, and Ca/P ratios of 2.06 and 2.31, for femur bone HAP and rib bone HAP respectively. After 20 kGy radiation exposure, however, these ratios were reduced.
- The FT-IR spectrum showed that the vibrational structure of the PO3-3 was slightly shifted due to the presence of a crack with the dose rate.
- The experimental mass attenuation coefficients of hydroxyapatite, originating from the bovine femur and rib bones, were computed as E= 511keV, 662keV, and 1276keV γ-ray energies. After 20 kGy irradiation, by way of 137Cs γ-ray point sources, the rib bone hydroxyapatite value shrank from 0.04 to 0.014 cm^2/gm, while the femur bone hydroxyapatite value was reduced from 0.031 to 0.011 cm^2/gm. for hydroxyapatite originating from the femur bone.

The findings, from this investigation, indicate that γ–ray radiation instigates flaws in the material of hydroxyapatite, as well as a reduction in the mass attenuation coefficient of the hydroxyapatite, derived from bovine femur and rib bones. It is our view that the significant loss in bone mineral density and Ca/P ratio, stemming from the exposure to 20 kGy ionizing radiation, could be at a level that can initiate the onset of osteoporosis.

Acknowledgments

The University of Salahaddin-Erbil is gratefully acknowledged for supporting the research activities and the reported results, we also thank Sarbast M. Ahmed from HMU for IR technical

support, we finally warmly thank the Soran University for EDX and SEM technical support.

Funding

Open Access funding enabled and organized by Salahaddin University-Erbil.

Declarations

Conflict of interest the authors declare no conflicts of interest.

Data availability statement

The data presented in this study are available on request from the corresponding author.

Author contributions

R. H. and S. K. conceived of the presented idea and wrote the manuscript, R. H. carried out the experiment, S. K. applied NIST XCOM program for an assessment of the test result. M. H. supervised the project. All authors discussed the results and contributed to the final manuscript

Ethical approval

We wish to declare that, this research ethically approved by Animal Research Ethics Committee (AREC), college of science, salahaddin university.

REFERENCES

AGRAWAL, K., SINGH, G., PURI, D. & PRAKASH, S. 2011. Synthesis and characterization of hydroxyapatite powder by sol-gel method for biomedical application. *J. Miner. Mater. Charact. Eng,* 10**,** 727-734.

AJITH KUMAR, B., NAVEEN KUMAR, K. & PRAKASH, T. J. M. C. 2023. Direct conversion x-ray sensing nanocomposite Ca10 (PO4) 6 (OH) 2: AgBiS2 for low-dose x-rays. *MRS Communications,* 13**,** 143-149.

AKAR, A., BALTAŞ, H., ÇEVIK, U., KORKMAZ, F. & OKUMUŞOĞLU, N. 2006. Measurement of attenuation coefficients for bone, muscle, fat and water at 140, 364 and 662 keV γ-ray energies. *Journal of Quantitative Spectroscopy and Radiative Transfer,* 102**,** 203-211.

AKÇA, B., ULUSOY, Ö., ERZENEOĞLU, S. Z. J. A. J. F. S. & ENGINEERING 2022. Total Mass Attenuation Coefficients, Total Photon Interaction Cross Sections, Effective Atomic Numbers and Effective Electron Densities for Some Construction Materials Available in Turkey. *Arabian Journal for Science and Engineering,* 47**,** 7479-7486.

AKRAM, M., AHMED, R., SHAKIR, I., IBRAHIM, W. A. W. & HUSSAIN, R. 2014. Extracting hydroxyapatite and its precursors from natural resources. *Journal of Materials Science,* 49**,** 1461-1475.

AMENAGHAWON, A. N., ANYALEWECHI, C. L., DARMOKOESOEMO, H. & KUSUMA, H. S. J. J. O. E. M. 2022. Hydroxyapatite-based adsorbents: Applications in sequestering heavy metals and dyes. *Journal of Environmental Management,* 302**,** 113989.

AMINI, M., NOGHREIYAN, A. V., DEHGHANI, Z. & ARA, M. H. M. 2018. Effect of gamma irradiation on the structure characteristics and mass attenuation coefficient of MgO nanoparticles. *Radiochimica Acta,* 106**,** 857-864.

BALATSOUKAS, I., KOURKOUMELIS, N. & TZAPHLIDOU, M. 2010. Auger electron spectroscopy for the determination of sex and age related Ca/P ratio at different bone sites. *Journal of Applied Physics,* 108**,** 074701.

BANO, N., JIKAN, S. S., BASRI, H., BAKAR, S. A. A. & NUHU, A. H. 2017. Natural hydroxyapatite extracted from bovine bone. *Journal of Science and Technology,* 9.

BARAKAT, N. A., KHIL, M. S., OMRAN, A., SHEIKH, F. A. & KIM, H. Y. 2009. Extraction of pure natural hydroxyapatite from the bovine bones bio waste by three different methods. *Journal of materials processing technology,* 209**,** 3408-3415.

BERGER, M. J. & HUBBELL, J. H. 1987. XCOM: Photon cross sections on a personal computer. National Bureau of Standards, Washington, DC (USA). Center for Radiation ….

BOGDANOVICIENE, I., BEGANSKIENE, A., TÕNSUAADU, K., GLASER, J., MEYER, H.-J. & KAREIVA, A. J. M. R. B. 2006. Calcium hydroxyapatite, Ca10 (PO4) 6 (OH) 2 ceramics prepared by aqueous sol–gel processing. 41**,** 1754-1762.

BORKOWSKI, L., PRZEKORA, A., BELCARZ, A., PALKA, K., JOZEFACIUK, G., LÜBEK, T., JOJCZUK, M., NOGALSKI, A. & GINALSKA, G. 2020. Fluorapatite ceramics for bone tissue regeneration: Synthesis, characterization and assessment of biomedical potential. *Materials Science and Engineering: C,* 116**,** 111211.

DEHGHANI, Z., NOGHREIYAN, A. V., NADAFAN, M. & ARA, M. M. 2018. The effect of different doses of γ–ray irradiation on the third order nonlinear optical properties, molecular structure and mass attenuation coefficients of synthesized colloidal silver nanoparticles. *Physica E: Low-dimensional Systems and Nanostructures,* 103**,** 423-429.

FIUME, E., MAGNATERRA, G., RAHDAR, A., VERNÉ, E. & BAINO, F. J. C. 2021. Hydroxyapatite for biomedical applications: A short overview. *Ceramics,* 4**,** 542-563.

FORERO-SOSSA, P., SALAZAR-MARTÍNEZ, J., GIRALDO-BETANCUR, A., SEGURA-GIRALDO, B. & RESTREPO-PARRA, E. J. S. R. 2021. Temperature effect in physicochemical and bioactive behavior of biogenic hydroxyapatite obtained from porcine bones. *Scientific Reports,* 11**,** 11069.

GEORGE, S., MEHTA, D. & SAHARAN, V. K. J. R. I. C. E. 2020. Application of hydroxyapatite and its modified forms as adsorbents for water defluoridation: an insight into process synthesis. *Reviews in Chemical Engineering,* 36**,** 369-400.

GHEDJEMIS, A., AYECHE, R. & BENOUADAH, A. J. J. O. T. A. C. S. 2022. A comparative study on

physicochemical properties of hydroxyapatite powder prepared from bovine and dromedary bone. 58**,** 607-616.

GIRIJA, E., PARTHIBAN, S. P., SUGANTHI, R., ELAYARAJA, K., JOSHY, M., VANI, R., KULARIA, P., ASOKAN, K., KANJILAL, D. & YOKOGAWA, Y. 2008. High energy irradiation——a tool for enhancing the bioactivity of Hydroxyapatite. *Journal of the Ceramic Society of Japan,* 116**,** 320-324.

GOMES, A. D., DE OLIVEIRA, A. A., HOUMARD, M. & NUNES, E. H. 2021. Gamma sterilization of collagen/hydroxyapatite composites: Validation and radiation effects. *Applied Radiation and Isotopes,* 174**,** 109758.

GUNDUZ, O., ERKAN, E. M., DAGLILAR, S., SALMAN, S., AGATHOPOULOS, S. & OKTAR, F. N. 2008. Composites of bovine hydroxyapatite (BHA) and ZnO. *Journal of Materials Science,* 43**,** 2536-2540.

HUBBELL, J. H. & SELTZER, S. M. 1995. Tables of X-ray mass attenuation coefficients and mass energy-absorption coefficients 1 keV to 20 MeV for elements Z= 1 to 92 and 48 additional substances of dosimetric interest. National Inst. of Standards and Technology-PL, Gaithersburg, MD (United ….

KAMINSKI, A., JASTRZEBSKA, A., GRAZKA, E., MAROWSKA, J., GUT, G., WOJCIECHOWSKI, A. & UHRYNOWSKA-TYSZKIEWICZ, I. 2012. Effect of gamma irradiation on mechanical properties of human cortical bone: influence of different processing methods. *Cell and tissue banking,* 13**,** 363-374.

KIEN, P. T., PHU, H. D., LINH, N. V. V., QUYEN, T. N. & HOA, N. T. J. N. B. F. R. M. 2018. Recent trends in hydroxyapatite (HA) synthesis and the synthesis report of nanostructure HA by hydrothermal reaction. 343-354.

KOKSAL, O., APAYDıN, G., TOZAR, A., KARAHAN, İ. H. & CENGIZ, E. 2019. Assessment of the mass attenuation parameters with using gamma-rays for manganese substituted nano hydroxyapatite. *Radiation Physics and Chemistry,* 159**,** 76-80.

KOURKOUMELIS, N., ZHANG, X., LIN, Z. & WANG, J. 2019. Fourier transform infrared spectroscopy of bone tissue: Bone quality assessment in preclinical and clinical applications of osteoporosis and fragility fracture. *Clinical Reviews in Bone and Mineral Metabolism,* 17**,** 24-39.

LONDOÑO-RESTREPO, S. M., RAMIREZ-GUTIERREZ, C. F., DEL REAL, A., RUBIO-ROSAS, E. & RODRIGUEZ-GARCÍA, M. E. 2016. Study of bovine hydroxyapatite obtained by calcination at low heating rates and cooled in furnace air. *Journal of materials science,* 51**,** 4431-4441.

MALLA, K. P., REGMI, S., NEPAL, A., BHATTARAI, S., YADAV, R. J., SAKURAI, S. & ADHIKARI, R. 2020. Extraction and characterization of novel natural hydroxyapatite bioceramic by thermal decomposition of waste ostrich bone. *International journal of biomaterials,* 2020.

MAMEDE, A. P., GONÇALVES, D., MARQUES, M. P. M. & BATISTA DE CARVALHO, L. A. 2018. Burned bones tell their own stories: A review of methodological approaches to assess heat-induced diagenesis. *Applied Spectroscopy Reviews,* 53**,** 603-635.

MARCUCCI, G., BELTRAMI, G., TAMBURINI, A., BODY, J., CONFAVREUX, C., HADJI, P., HOLZER, G., KENDLER, D., NAPOLI, N. & PIERROZ, D. J. A. O. O. 2019. Bone health in childhood cancer: review of the literature and recommendations for the management of bone health in childhood cancer survivors. *Annals of Oncology,* 30**,** 908-920.

MORE, C. V., LOKHANDE, R. M. & PAWAR, P. P. 2016. Effective atomic number and electron density of amino acids within the energy range of 0.122–1.330 MeV. *Radiation Physics and Chemistry,* 125**,** 14-20.

ODUSOTE, J. K., DANYUO, Y., BARUWA, A. D. & AZEEZ, A. A. 2019. Synthesis and characterization of hydroxyapatite from bovine bone for production of dental implants. *Journal of applied biomaterials & functional materials,* 17**,** 2280800019836829.

OOI, C., HAMDI, M. & RAMESH, S. 2007. Properties of hydroxyapatite produced by annealing of bovine bone. *Ceramics international,* 33**,** 1171-1177.

OSUCHUKWU, O. A., SALIHI, A., ABDULLAHI, I., ABDULKAREEM, B. & NWANNENNA, C. S. J. S. A. S. 2021. Synthesis techniques, characterization and mechanical properties of natural derived hydroxyapatite scaffolds for bone implants: A review. 3**,** 1-23.

PREDOI, D., CIOBANU, C. S., ICONARU, S. L., PREDOI, S. A., CHIFIRIUC, M. C., RAAEN, S., BADEA, M. L. & ROKOSZ, K. 2022. Impact of Gamma Irradiation on the Properties of Magnesium-Doped Hydroxyapatite in Chitosan Matrix. *Materials,* 15**,** 5372.

RAFIEI, M. M., PARSAEI, S., KAUR, P., SINGH, K., BÜYÜKYıLDıZ, M., KURUDIREK, M. J. B. P. & EXPRESS, E. 2022. A Monte Carlo investigation of some important radiation parameters and tissue equivalency for photons below 1 keV in human tissues. *Biomedical Physics & Engineering Express,* 8**,** 025002.

RAHMAN, N., KHAN, R. & BADSHAH, S. 2018. Effect of x-rays and gamma radiations on the bone mechanical properties: literature review. *Cell and Tissue Banking,* 19**,** 457-472.

RANA, M. M., AKHTAR, N., RAHMAN, M., HASAN, M. Z. & ASADUZZAMAN, S. 2017. Extraction and characterization of hdroxyapatite from bovine cortical bone and effect of radiatio. *International Journal of Biosciences,* 11**,** 20-30.

SALCEDO, M. P., SOOD, A. K., JHINGRAN, A., EIFEL, P. J., KLOPP, A. H., IYER, R. B., FELLMAN, B. M., JIMENEZ, C. & SCHMELER, K. M. J. C. 2020. Pelvic fractures and changes in bone mineral density after radiotherapy for cervical, endometrial, and vaginal cancer: a prospective study of 239 women. *Cancer,* 126**,** 2607-2613.

SIDHU, B. S., DHALIWAL, A., MANN, K. & KAHLON, K. 2012. Study of mass attenuation coefficients, effective atomic numbers and electron densities for some low Z compounds of dosimetry interest at 59.54 keV incident photon energy. *Annals of Nuclear Energy,* 42**,** 153-157.

SINGH, K., KAUR, G., KUMAR, V., DHAMI, A. & LARK, B. 1998. Measurement of attenuation coefficients of some dilute solutions at 662 keV. *Radiation Physics and Chemistry,* 53**,** 123-126.

SOBCZAK-KUPIEC, A. & WZOREK, Z. 2012. The influence of calcination parameters on free calcium oxide content in natural hydroxyapatite. *Ceramics International,* 38**,** 641-647.

TARIQ, U., HAIDER, Z., HUSSAIN, R., TUFAIL, K. & ALI, J. LIBS analysis of hydroxyapatite extracted from bovine bone for Ca/P ratio measurements. AIP Conference Proceedings, 2017. AIP Publishing LLC, 030027.

TIWARI, P. & MISHRA, K. P. J. I. J. O. R. B. 2020. Flavonoids sensitize tumor cells to radiation: molecular mechanisms and relevance to cancer radiotherapy. 96**,** 360-369.

UNAL, S., OKTAR, F. N., MAHIROGULLARI, M. & GUNDUZ, O. 2021. Bone structure and formation: A new perspective. *Bioceramics.* Elsevier.

WANG, Q., LI, W., LIU, R., ZHANG, K., ZHANG, H., FAN, S. & WANG, Z. 2019. Human and non-human bone identification using FTIR spectroscopy. *International journal of legal medicine,* 133**,** 269-276.

YAZDANI DARKI, S., KESHAVARZ, S. J. N. S. & TECHNIQUES 2020. Studies on mass attenuation coefficients for some body tissues with different medical sources and their validation using Monte Carlo codes. *Nuclear Science and Techniques,* 31**,** 119.

YELTEN-YILMAZ, A. & YILMAZ, S. J. C. I. 2018. Wet chemical precipitation synthesis of hydroxyapatite (HA) powders. 44**,** 9703-9710.